PHYSICAL REVIEW LETTERS

Observation of Spatially Coherent Polarization Vector Fields and Visualization of Vector Singularities

Y. F. Chen,* T. H. Lu, and K. F. Huang

Department of Electrophysics, National Chiao Tung University, Hsinchu, Taiwan, Republic of China
(Received 6 September 2005; published 23 January 2006)

We present experimental observations of polarization vector fields from a highly isotropic microchip laser with a large Fresnel number. The experimental polarization vector field leads to complex entanglement of spatial structures and polarization states. We theoretically derive the representation of generalized coherent states to reconstruct the experimental polarization-resolved patterns. The analytical and precise reconstruction enables the vector singularities to be clearly visualized.

Recent rapid advances in technology have driven a critical inspection of coherent wave properties in mesoscopic physics. Phase singularities in scalar waves, known as wave front dislocations, play an important role in modern physics, and are observed in quantum and microwave billiards [1], quantum ballistic transport [2], linear and nonlinear optics [3], and superconducting films [4], symmetrically confined superfluids and Bose-Einstein condensates [5], and liquid crystal films [6]. Currently, interest is focused not only on the phase singularities but also on the polarization singularities, known as wave front disclinations [7]. As pointed out by Freund [8], there are two types of singularities of the polarization vectors of paraxial optical beams: vector singularities and Stokes singularities. Vector singularities are isolated, stationary points in a plane at which the orientation of the electric vector of a linearly polarized vector field becomes undefined. The nature of the vector singularities has been studied in coherent optical waves with the correlated behavior of spatial structures and polarization state [9]. However, the experimental observations were almost restricted to low-order transverse modes [10]. Until now there has been no experimental evidence of vector singularities involving the entanglement of polarization and spatial structures in high-order Gaussian beams.

Recently, a diode-pumped microchip laser has been employed to perform analogous studies of coherent phenomenon in scalar waves [11]. In this Letter, we demonstrate experimental observations of polarization singularities from a highly isotropic microchip laser with a large Fresnel number. The experimental polarization vector field is found to be made up of two linearly polarized modes with different spatial structures that are phase synchronized to a single frequency. With the extension of the SU(2) coherent states, we analytically reconstruct the two orthogonally polarized spatial structures and display the formation of vector singularities in a perceptible way.

In this experiment, the laser system is a diode-pumped Nd:YVO$_4$ microchip laser with a ring-shaped pump profile. The resonator configuration is basically similar to that used in Ref. [12]. Since the YVO$_4$ crystal belongs to the group of oxide compounds crystallizing in a Zircon structure with tetragonal space group, the Nd-doped YVO4 crystals show strong polarization dependent fluorescence emission due to the anisotropic crystal field. The fourfold symmetry axis of the YVO$_4$ crystal is the crystallographic c axis; perpendicular to this axis are the two indistinguishable a and b axes. Therefore, our Nd:YVO$_4$ crystal is precisely cut along the c axis for high-level transverse isotropy. It is worthwhile to note that our gain medium is different from the conventional Nd:YVO$_4$ crystals that are cut along the a axis to use the largest stimulated emission cross section for lowering the lasing threshold. The transverse patterns are measured with a CCD camera and an optical spectrum analyzer is used to monitor the laser spectra.

Experimental results reveal that the transverse patterns were localized on the elliptic orbits when we used an output coupler with the reflectivity of 98% in the laser cavity [12]. However, the transverse patterns were usually the extended structures restricted by the hyperbolic caustics when we used an output coupler with the reflectivity of 99%. A noteworthy finding is that adjusting the pump beam delicately can generate the lasing modes to be made up of two distinct hyperbolic patterns with orthogonal linear polarization. In other words, the transverse pattern is linearly polarized, but the polarization is spatially dependent. Figures 1(a)–1(d) show the experimental polarization-resolved patterns in the 0°, 45°, 90°, and 135° direction. It is found that the entanglement of spatial structures and polarization states forms an optical vector field and leads to the transverse patterns to be polarization dependent. The basic requirement for a vector polarization pattern is that the orthogonal polarization modes with different spatial patterns are phase synchronized to a common frequency. The measurement of the optical spectrum verifies that the observed transverse pattern is phase synchronized to a single frequency at 1064 nm. We believe that the present experiment provides the first observation of a vector pattern involving the high-order Gaussian beams. Since direct measurements of polarization vector filed are currently not feasible, we focus on deriving the analytic
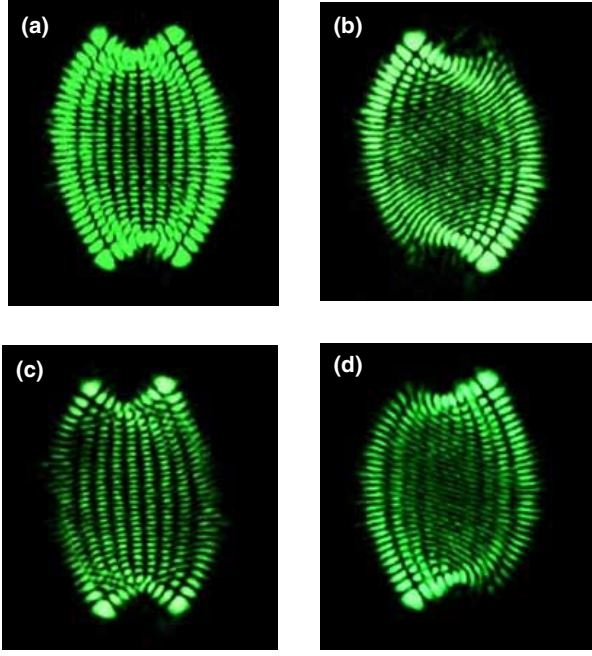
033901-1

FIG. 1 (color online). Experimental polarization-resolved patterns (a) 0° polarization, (b) 45° polarization, (c) 90° polarization, and (d) 135° polarization.

representation for the wave functions of experimental hyperbolic patterns to visualize the polarization vector filed. Although the nodal-line structures of the experimental hyperbolic patterns are somewhat similar to that of eigenstates in the elliptic quantum billiard [13], the confinement conditions for both systems are utterly different. So far, the wave functions for the hyperbolic modes in the spherical resonators have not been explicitly explored.

The wave functions for the paraxial fields in the spherical resonators can be expressed as Hermite-Gaussian (HG) function with Cartesian symmetry $\Phi_{m,n}^{HG}(x, y, z)$, where m and n are the indices of x and y coordinates or Laguerre-Gaussain (LG) function with cylindrical symmetry $\Phi_{p,l}^{LG}(r, \phi, z)$, where p and l are the radial and azimuthal indices [14]. It is well known that the paraxial wave equation for the spherical resonators has the identical form with the Schrödinger equation for the two-dimensional (2D) harmonic oscillator [14]. The SU(2) coherent states for the 2D harmonic oscillator are well localized on classical elliptic trajectories [15]. Not only in the 2D harmonic oscillator, the SU(2) coherent states have been shown to play a vital role for the quantum-classical connection in the 2D quantum systems [16]. In terms of the HG modes, the SU(2) coherent states for the elliptic modes are expressed as [15]

$$\Psi_N^{CS}(x, y, z; \varphi) = \frac{1}{\sqrt{2^N}} \sum_{K=0}^{N} \frac{\sqrt{N!}}{\sqrt{(N-K)!}\sqrt{K!}} \times e^{iK\varphi} \Phi_{N-K,K}^{HG}(x, y, z), \quad (1)$$

where the parameter φ is the relative phase between vari-

ous HG modes and is related to the eccentricity of the elliptic trajectory. As shown in a variety of integrable 2D quantum billiard systems, the phase factors φ in the SU(2) coherent states play an important role in the quantum-classical connection [16]. It has been confirmed that the experimental elliptic patterns agree very well with the SU(2) elliptic states [12]. From Eq. (1), the coherent state $\Psi_N^{CS}(x, y, z; \varphi)$ with $\varphi = 0$ can be derived to be the diagonal HG mode $\Phi_{0,N}^{HG}(x', y', z)$, where $x' = (x + y)/\sqrt{2}$ and $y' = (x - y)/\sqrt{2}$. On the other hand, the coherent state $\Psi_N^{CS}(x, y, z; \varphi)$ can be transformed into the LG mode $\Phi_{0,N}^{LG}(r, \phi, z)$ when $\varphi = \pi/2$. Briefly, the SU(2) elliptic mode is transformed from a diagonal HG mode $\Phi_{0,N}^{HG}(x', y', z)$ into a LG mode $\Phi_{0,N}^{LG}(r, \phi, z)$ when the phase factor φ varies from 0 to $\pi/2$.

The SU(2) coherent states can only be used to describe the elliptic patterns. To explain the experimental hyperbolic patterns, we develop the generalized coherent states (GCSs) to be related to the transformation from a diagonal HG mode $\Phi_{p,p+l}^{HG}(x', y', z)$ into a LG mode $\Phi_{p,l}^{LG}(r, \phi, z)$ with a phase factor φ. Mathematically, the diagonal HG mode $\Phi_{p,p+l}^{HG}(x', y', z)$ can be expressed by a summation of nonrotated HG modes $\Phi_{2p+l-k,k}^{HG}(x, y, z)$ with $k = 0, 1, 2, \ldots, 2p + l$: [17]

$$\Phi_{p,p+l}^{HG}(x', y', z) = \sum_{k=0}^{2p+l} B(p, l, k)\Phi_{2p+l-k,k}^{HG}(x, y, z) \quad (2)$$

with

$$B(p, l, k) = \frac{(-1)^k}{\sqrt{2^{2p+l}}} \sum_s \frac{(-1)^s \sqrt{(p+l)!p!(2p+l-k)!k!}}{s!(k-s)!(p+l-s)!(p-k-s)!},$$
$$(3)$$

where the summation over s is taken whenever none of the arguments of factorials in the denominator are negative. From Eq. (2), successive HG modes $\Phi_{2p+l-k,k}^{HG}(x, y, z)$ of the summation can be found to be in phase. In a similar way, any LG modes $\Phi_{p,l}^{LG}(r, \phi, z)$ can be decomposed into a sum of HG modes $\Phi_{2p+l-k,k}^{HG}(x, y, z)$ with the same coefficients $B(p, l, k)$ but an additional $\pi/2$ phase factor:

$$\Phi_{p,l}^{LG}(r, \phi, z) = \sum_{k=0}^{2p+l} e^{ik(\pi/2)} B(p, l, k)\Phi_{2p+l-k,k}^{HG}(x, y, z).$$
$$(4)$$

As in the representation of SU(2) coherent states, we utilize the phase factor φ to characterize a new family of GCSs:

$$\Psi_{p,l}^{CS}(x, y, z; \varphi) = \sum_{k=0}^{2p+l} e^{ik\varphi} B(p, l, k)\Phi_{2p+l-k,k}^{HG}(x, y, z). \quad (5)$$

The GCSs in Eq. (5) exhibit a traveling-wave property. The standing-wave representation of the GCSs is given by

$$\begin{Bmatrix} \Psi_{p,l}^{\cos}(x,y,z;\varphi) \\ \Psi_{p,l}^{\sin}(x,y,z;\varphi) \end{Bmatrix} = \sqrt{2}\left[\sum_{k=0}^{2p+l} \begin{Bmatrix} \cos(k\varphi) \\ \sin(k\varphi) \end{Bmatrix} B(p,l,k)\Phi_{2p+l-k,k}^{\mathrm{HG}}(x,y,z) \right]. \tag{6}$$

The GCSs represent a general family to comprise the HG and LG mode families as special cases. More importantly, the GCSs with the particular phase factor can reveal the patterns with hyperbolic caustics. It is worthwhile to mention that the present GCSs are intimately correlated to the Hermite-Laguerre Gaussian (HLG) beams described by Abramochkin and Volostnikov [18]. The HLG modes are the superposition of HG modes with a fixed relative phase factor of $\pi/2$ but different amplitude factors, whereas the present GCSs are the superposition of HG modes with a set of fixed relative amplitude factors but different phase factors. Unlike the GCSs, the orientations of symmetrical axes of the HLG modes are rotated with the transformation. Although the HLG modes can be shown to be completely identical to the GCSs with a coordinate rotation about the origin, the representation of the GCSs is more elegant to interpret the experimental patterns.

We applied the GCSs to explain the experimental results and found that the observed vector pattern can be fittingly described as

$$\vec{E}(x,y,z) = \Psi_{4,30}^{\cos}(x',y',z;0.235\pi)\hat{x}$$
$$- [\Psi_{4,30}^{\sin}(x',y',z;0.235\pi)$$
$$+ \Psi_{3,32}^{\cos}(x',y',z;0.235\pi)]\hat{y}, \tag{7}$$

where $x' = (x+y)/\sqrt{2}$ and $y' = (-x+y)/\sqrt{2}$. Figure 2 depicts the numerically reconstructed patterns for the experimental results shown in Fig. 1. The good agreement between the reconstructed and experimental patterns confirms that the GCSs provide a realistic description for the
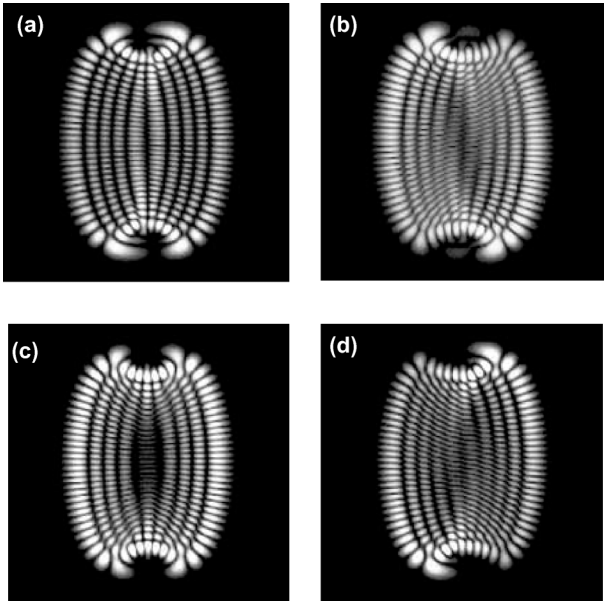
optical coherent waves in the mesoscopic regime. We use the analytical function given in Eq. (7) to visualize the experimental polarization vector pattern. Figure 3 displays the numerically calculated polarization vector field for the observed pattern, where different colors are used to highlight the polarization directions. It is seen that the polarization vector field exhibits a complex interlace pattern. The polarization vector fields for two small regions are also plotted to visualize the fine details of the polarization singularities. The polarization streamlines around the singularities generally display swirling features. To our knowledge, polarization singularities involving the high-order Gaussian beam are analyzed and visualized for the first time.

Vector point singularities are conventionally described in terms of the phase field $\Theta(x,y) = \arctan(E_y/E_x)$, where E_x and E_y are the scalar components of the vector field $\vec{E}$ along the x and y axes. The vortices of $\Theta(x,y)$ are the vector singularities at which the orientation of the vector of $\vec{E}$ is undefined. An essential constraint obeyed by vector singularities is the sign rule that adjacent singularities on any contour of constant phase must have opposite signs [19]. Figure 4 depicts the contour plot of phase field $\Theta(x,y)$ for the boxed regions shown in Fig. 3 to confirm the sign rule. From Fig. 4, it can be also found that all saddle points are to be open saddles with no joined arms. Since no closed saddles are found in the experimental vector field, no phase extrema are observed. As discussed

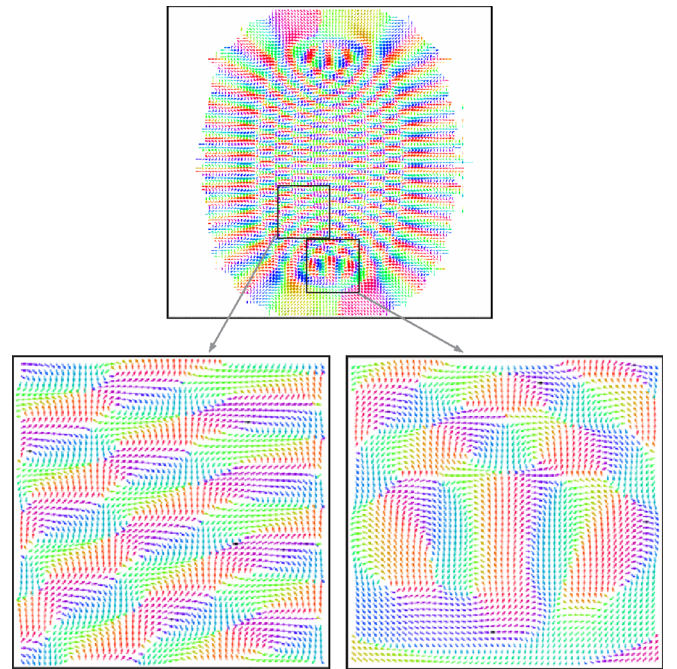FIG. 2.   Numerically reconstructed patterns for the experimental results shown in Fig. 1.

FIG. 3 (color online).   Numerically calculated polarization vector field for the observed patterns.
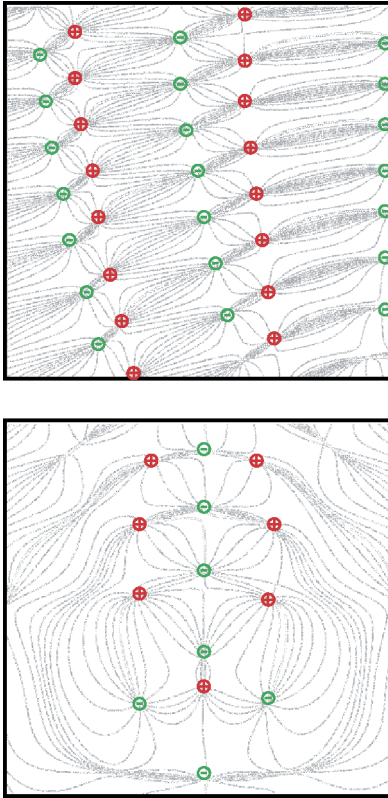
FIG. 4 (color online). Contour plot of phase field $\Theta(x, y)$ for the boxed regions shown in Fig. 3 to confirm the sign rule. Positive and negative index singularities are labeled by their signs + and −, respectively.

in Ref. [19], the phase extrema are really rare because there is little room left in the phase field to accommodate them.

In summary, we have used a highly isotropic microchip laser with a large Fresnel number to generate a polarization vector field. With the representation of the SU(2) coherent state, we have originally developed the GCSs to reconstruct the experimental observation and to visualize the polarization vector singularities in a manifest way. The present results indicate that the GCSs constitute a useful family of quantum states for the 2D harmonic oscillator with spin-orbit interactions.

---

*Email address: yfchen@cc.nctu.edu.tw
Tel: (886-35) 712121 ext. 56106
Fax: (886-35) 729134

[1] P. Šeba, U. Kuhl, M. Barth, and H. J. Stöckmann, J. Phys. A **32**, 8225 (1999).
[2] K. F. Berggren, A. F. Sadreev, and A. A. Starikov, Phys. Rev. E **66**, 016218 (2002).
[3] J. F. Nye and M. V. Berry, Proc. R. Soc. A **336**, 165 (1974); P. Coullet, L. Gil, and J. Lega, Phys. Rev. Lett. **62**, 1619 (1989); F. T. Arecchi, G. Giacomelli, P. L. Ramazza, and S. Residori, Phys. Rev. Lett. **67**, 3749 (1991); N. Shvartsman and I. Freund, Phys. Rev. Lett. **72**, 108 (1994); W. Wang, S. G. Hanson, Y. Miyamoto, and M. Takeda, Phys. Rev. Lett. **94**, 103902 (2005).
[4] L. F. Chibotaru, A. Ceulemans, V. Bruyndoncx, and V. V. Moshchalkov, Phys. Rev. Lett. **86**, 1323 (2001); B. J. Baelus and F. M. Peeters, Phys. Rev. B **65**, 104515 (2002).
[5] E. L. Andronikashvili and Y. G. Mamaladze, Rev. Mod. Phys. **38**, 567 (1966); K. W. Madison, F. Chevy, W. Wohlleben, and J. Dalibard, Phys. Rev. Lett. **84**, 806 (2000).
[6] P. G. de Gennes and J. Prost, *The Physics of Liquid Crystals* (Oxford University Press, New York, 1993), 2nd ed.
[7] J. F. Nye, Proc. R. Soc. A **387**, 105 (1983); M. Soskin, V. Denisenko, and R. Egorov, J. Opt. A Pure Appl. Opt. **6**, S281 (2004).
[8] I. Freund, Opt. Commun. **199**, 47 (2001).
[9] L. Gil, Phys. Rev. Lett. **70**, 162 (1993); T. Erdogan, Appl. Phys. Lett. **60**, 1921 (1992); Y. F. Chen, K. Huang, H. C. Lai, and Y. P. Lan, Phys. Rev. Lett. **90**, 053904 (2003); I. V. Veshneva, A. I. Konukhov, L. A. Melnikov, and M. V. Ryabinina, J. Opt. B **3**, S209 (2001).
[10] F. Prati, G. Tissoni, M. S. Miguel, and N. B. Abraham, Opt. Commun. **143**, 133 (1997).
[11] Y. F. Chen, C. H. Jiang, Y. P. Lan, and K. F. Huang, Phys. Rev. A **69**, 053807 (2004); Y. F. Chen, Y. P. Lan, and K. F. Huang, Phys. Rev. A **68**, 043803 (2003).
[12] Y. F. Chen and Y. P. Lan, Phys. Rev. A **66**, 053812 (2002); Phys. Rev. A **67**, 043814 (2003).
[13] H. Waalkens, J. Wiersig, and H. R. Dullin, Ann. Phys. (N.Y.) **260**, 50 (1997).
[14] H. Kogelnik and T. Li, *Proceedings of the IEEE 54*, (IEEE, Piscataway, 1966), pp. 1312–1329.
[15] V. Bužek and T. Quang, J. Opt. Soc. Am. B **6**, 2447 (1989); J. Banerji and G. S. Agarwal, Opt. Express **5**, 220 (1999).
[16] Y. F. Chen and K. F. Huang, Phys. Rev. E **68**, 066207 (2003); Y. F. Chen, Y. P. Lan, and K. F. Huang, Phys. Rev. E **66**, 066210 (2002).
[17] E. Abramochkin and V. Volostnikov, Opt. Commun. **83**, 123 (1991).
[18] E. G. Abramochkin and V. G. Volostnikov, J. Opt. A Pure Appl. Opt. **6**, S157 (2004).
[19] I. Freund, Phys. Rev. E **52**, 2348 (1995); M. S. Soskin, V. Denisenko, and I. Freund, Opt. Lett. **28**, 1475 (2003).